

ENteric Immunity SIMulator: A tool for *in silico* study of gut immunopathologies

Katherine V. Wendeldorf^{*§}, Josep Bassaganya-Riera^{†§}, Keith Bisset^{*§}, Stephen Eubank^{*§},
Raquel Hontecillas^{†§} and Madhav Marathe[‡]

^{*}Network Dynamics and Simulation Science Laboratory

[†]Nutritional Immunology and Molecular Medicine Laboratory

[‡]Department of Computer Science

[§]Center for Modeling Immunity to Enteric Pathogens

Virginia Bioinformatics Institute, Virginia Polytechnic Institute and University

Washington Street, MC 0477 Blacksburg, Virginia 24061 USA

Email: wkath83@vbi.vt.edu, jbasaga@vbi.vt.edu, kbisset@vt.edu, seubank@vbi.vt.edu, rmagarzo@vbi.vt.edu, mmarathe@vbi.vt.edu

Abstract—Clinical symptoms of gastrointestinal (GI) infections are often caused by the inflammatory response elicited to eliminate the invading microbe. Here we present ENISI, a simulator of GI immune mechanisms in response to resident commensal bacteria as well as invading pathogens and the effect on host clinical symptoms. ENISI is a tool for identifying treatment strategies that reduce inflammation-induced damage and, at the same time, ensure pathogen removal by allowing one to test plausibility of *in vitro* observed behavior as explanations for observations *in vivo*, propose behaviors not yet tested *in vitro* that could explain these tissue-level observations, and conduct low-cost, preliminary experiments of proposed interventions/treatments.

An example of such application is shown in which we simulate dysentery resulting from *B. hyodysenteriae* infection and identify aspects of the host immune pathways that lead to continued inflammation-induced tissue damage even after pathogen elimination.

I. INTRODUCTION

Enteric diseases are diseases of the gastrointestinal (GI) tract often caused by ingestion of microbes in food and water. Upon microbe entry immune cells in the GI tract mount an inflammatory response that eliminates the microbe, but may also cause tissue damage. This collateral damage is often the basis of various clinical symptoms including lesions of the epithelial lining and bloody diarrhea.

As the GI tract is constantly exposed to foreign antigens, mostly innocuous, this inherent inflammatory response must be regulated so that the system does not remain in a constant state of tissue-damaging hyper-inflammation. This is carried out by the *regulatory*, or anti-inflammatory, immune response triggered by factors such as host tissue damage or commensal bacteria of the gut microflora. The current picture of the gut mucosa is one in which immune cells of the regulatory and inflammatory responses are in constant competition, with regulatory phenotypes generally predominating [7], [11]. Understanding which components of these immune pathways

contribute to microbial persistence and severity of symptoms is necessary to devise treatments and infection prevention strategies against gut pathogens such as *E. coli* and *H. pylori*.

Here we present ENISI, a simulator of the inflammatory and regulatory immune pathways initiated by microbe-immune cell interactions in the gut. With ENISI mucosal immunologists can test and generate hypotheses for enteric disease pathology and propose interventions through experimental infection of an *in silico* gut. This is done by using a simple scripting language to assign parameter values that conform to one's knowledge and assumptions of the experimental scenario they wish to simulate. Simulation outcomes given different experimental conditions allow observation of *in silico* behaviors that are not readily seen through *in vitro* and *in vivo* techniques. This information can then be used to generate novel treatment strategies that can be tested in the laboratory.

A. Mucosal inflammatory and regulatory immune pathways

Here we describe the specific inflammatory and regulatory immune pathways encoded in ENISI as shown in Figure 1.

The mammalian gut mucosa can be divided into three sites: *i*) the *Lumen*, which has a direct connection to the external environment, is the entry site for ingested food and foreign microbes, and houses gut microflora, *ii*) the *Lamina propria* (LP), tissue separated from the lumen by an epithelial monolayer that is occupied by resting immune cells, *iii*) the epithelial barrier (EB), a monolayer of epithelial cells, that divides the lumen and LP.

The events of inflammatory immune pathways (red lines) are as follows with numbers corresponding to those labeling the events depicted in Figure 1: (1) A pathogen, such as foreign bacteria, enters the lumen and contacts the EB. (2) Intestinal epithelial cells (EC) differentiate to a pro-inflammatory phenotype (pEC) either in response to damage caused by the pathogen or by mere recognition of the pathogen. The pEC phenotype secretes microbicides and various signalling chemicals (cytokines) and may be permeable allowing pathogen

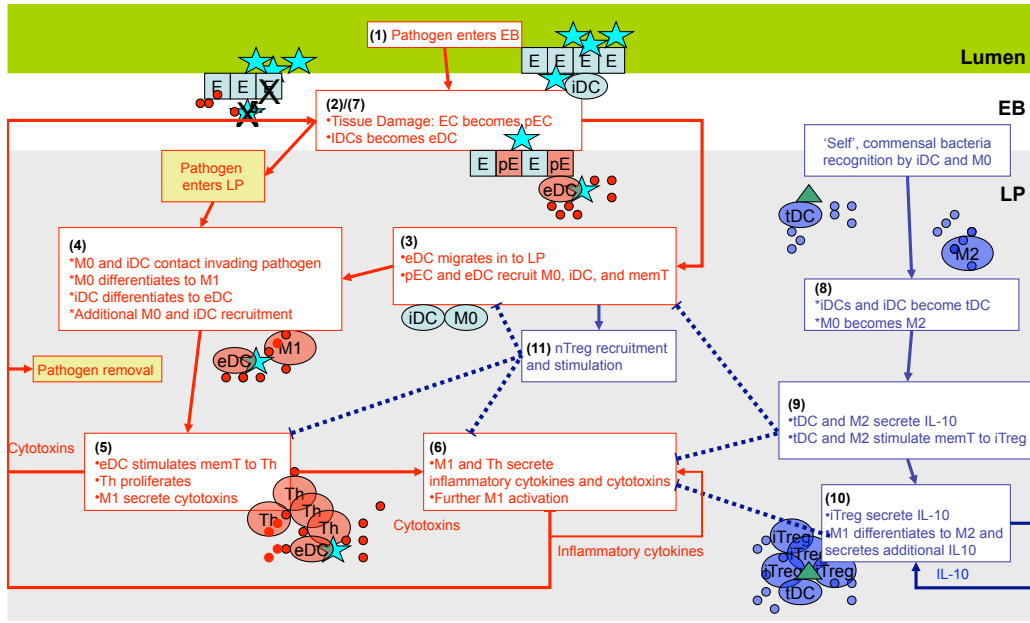


Fig. 1. Illustration of sequential events in the inflammatory (red arrows) and regulatory (blue arrows) pathways described in the text. Dashed lines indicate events that inhibit the occurrence of another event.

entry in to the LP [9]. At the same time, immature ‘sampling’ dendritic cells (iDCs), which reside in the EB and contact microbes in the lumen, internalize the pathogen and mature to an effector phenotype (eDC) that migrates in to the LP and presents components of the pathogen (antigen) on its surface. (3) Chemicals secreted by damaged epithelial cells and eDC recruit resting macrophages (M0) and dendritic cells (iDC). (4) These macrophages and dendritic cells may then contact and internalize pathogen that has entered the LP. This leads to maturation of iDC to an eDC phenotype and differentiation of macrophages to an inflammatory M1 phenotype. (5) Mature, antigen-presenting eDC go on to recruit resting CD4⁺ T cells (memT) to the LP and secrete cytokines such as IL-12 and IFN- γ that induce T cell differentiation to a pro-inflammatory Th1 or Th17 phenotype (Th) upon antigen recognition [11]. These stimulated T cells enter a transient state of proliferation, each giving rise to approximately 500 daughter cells of the same phenotype. M1 go on to secrete cytotoxic proteases and radicals that kill surrounding microbes as well host epithelial cells. (6) Th1/Th17 cells secrete cytotoxins and cytokines that enhance secretion of inflammatory factors by surrounding T cells as well as induce additional macrophages to a M1 phenotype (7) The epithelial cells damaged by Th1/Th17 and M1 secreted factors then respond by secreting additional inflammatory cytokines resulting in more immune cell recruitment along with openings in the epithelial barrier that can allow direct pathogen entry into the LP at which point recruited M0 and iDC are activated to inflammatory phenotypes. This completes a positive, inflammatory feedback loop. Inflammation generally dissipates when pathogen is eliminated and direct immune cell stimulation ceases.

The anti-inflammatory, regulatory pathway is composed of

the following events: Dendritic cells and macrophages contact self-antigen or commensal bacteria that reside in the lumen or has invaded the LP through the damaged epithelium. (8) Upon internalization of the commensal or self-antigen, dendritic cells differentiate to a tolerogenic phenotype (tDC) and macrophages differentiate to an M2 phenotype. (9) M2 and tDC go on to secrete the anti-inflammatory cytokine IL-10. IL-10 reduces inflammatory cytokine and cytotoxin production in surrounding immune cells, dampening the inflammatory loop. They also present the tolerance-inducing antigen to CD4⁺ T cells inducing their differentiation to T regulatory cells (iTreg). (10) iTreg goes on to secrete additional IL-10. The increase in environmental IL-10 induces differentiation of macrophages already of an inflammatory M1 phenotype to the regulatory M2 phenotype [7]. This promotes further IL-10 production and stimulation of T cells to iTreg closing a positive anti-inflammatory feedback loop.

(11) Another regulatory pathway involves *natural* T-regulatory cells (nTreg). These are T cells in the LP that are pre-destined to be regulatory cells independent of the phenotype of the presenting dendritic cell (eDC or tDC) or macrophage. nTreg may have a reduced proliferation capacity compared to conventional T cells. Like iTreg, nTreg secretes IL-10 promoting further M2 creation. In addition, nTreg bind eDC and inhibit their recruitment and stimulation of resting T cells to inflammatory phenotypes [19].

Certain genetic predispositions or immune dysfunctions can result in an inflammatory pathway being initiated by commensal bacteria strains [18].

II. ENISI

ENISI encodes each immune pathway as an agent-based model representing each individual cell that participates in

each component event. Individual cells are represented as a set of finite state automata $\langle c_1 \dots c_n \rangle$ each corresponding to an automaton that represents an **epithelial cell**, a **commensal bacteria**, a **foreign bacteria**, a **macrophage**, a **dendritic cell**, a **'sampling' dendritic cell** (sDC), a conventional CD4+ T cell (**T cell**), or a natural T-regulatory cell (**nTreg**) (Figure 2). Cell names written in bold text refer to the corresponding model automaton that represents the cell behavior in the system. 'Sampling' dendritic cells of the EB and dendritic cells that reside in the LP may have differing activation periods and responses to commensal bacteria [18], [9]. **Commensal bacteria** represent individual bacterium of the microbiota that are located in the lumen (*B_lumen*) and are endowed with behaviors assumed to be shared by most commensal strains. The cell-type of each individual is determined by its initial state.

The automata, representing individual cells, are assigned to one of three *Locations*; lumen, LP, and blood. *Locations*, are divided in to discrete patches, the *sublocations*, where a sublocation is defined as the maximum volume at which an individual can be assumed to be in contact with all other individuals in that sublocation. Individuals occupy and migrate between *Locations* according to a *schedule* assigned to each individual by their *state*. Cells occupy a different randomly chosen *sublocation* of the assigned *Location* at short time intervals representing random movement and resulting in a dynamic contact network, G .

The system is a Co-evolving Graphical Discrete Dynamical System (CGDDS), a 4-tuple $\beta = (G, S, F, R)$. G is a time varying graph that is the cell contact network, S is a set of states listed in Table I, and F is a set of functions that describes state transitions. Here, F is represented as the set of cell-specific automata that are probabilistic timed transition systems. R is an update scheme that determines the order in which automaton state transitions are computed and states of nodes in G are updated.

Each individual, c_i , occupies a state $s_i \in S$ that corresponds to either a cell's *phenotype*, the *Location* of the cell, or its status as *dead*. The state transition function f_i depends on the current state of the individual s_i and at least one of the following: *i*) the amount of time c_i has occupied its current state and *ii*) the states of its current contacts in the graph. For each state s there is a set of *Interactor* states I_s such that if a contact c_j of individual c_i is in a state $s_j \in I_{s_i}$, c_i will interact with c_j and probabilistically transition states. At any time t , the configuration $\xi(t)$ of a GDS is a vector $(s_1(t), s_2(t), \dots, s_n(t))$, where $s_i(t)$ represents the state of c_i at time t . The time evolution of a GDS is represented by the sequence of successive configurations of the GDS. The function for the interaction probability may be *single contact-dependent*, calculated in a pairwise manner, or *multicontact-dependent*, a function of the configuration of the subnetwork in the specific sublocation occupied by c_i . The set of functions, F , is formalized in a state chart like manner, described below in greater detail.

Upon a change of state, the individual may or may not be

assigned to a new *Location*. This contact-dependent transition may explicitly represent contact-dependent cell differentiation, such as the stimulation of resting T cells by dendritic cells, which requires surface-surface contact. Transitions may also implicitly represent differentiation induced by cytokines secreted by surrounding cells, as is the case for a $M1 \rightarrow M2$ transition, which is a function of the cytokine concentrations in the local environment.

Each *event* of the immune pathway is then defined by a specific state transition $s_i \rightarrow x$, where $x \in S$. For example, tissue damage occurs when one cell represented by an **epithelial cell** automaton makes the transition $EC \rightarrow pEcell$. A specific *health outcome* is a stable configuration of the system, ξ_s , following contact between one of the bacteria automata and one of the immune cell automata. The CGDDS formalism imposes various approximations described in detail in [21].

As a spatially explicit, agent-based model ENISI simulations take in to account spatial-temporal heterogeneity across individual cells and allow stochasticity in cell behavior in the form of probabilistic state transitions that are functions of tissue location, cell age, demographics of surrounding immune cells, and duration of contact with other immune cells and antigen. The method allows one to manipulate automaton transition criteria with a direct interpretation between changes in model rules and experimental modifications of cells. The net effect that arises from localized interactions is then the predicted outcome of the experimental system.

Users may modify rules to set experimental conditions by specifying any of the following features of the system: *i*) *Infection specifics*: dose and timing of pathogen entry; *ii*) *Experimental host phenotypes*: parameters governing interactions between specific phenotypes to represent changes in cytokine and cytokine-receptor expression; *iii*) *Host immunological set-point*: initial immune cell populations present at the time of infection; and *iv*) *Strain-specific functions of bacteria*: specifications of interaction conditions and consequences for **commensal bacteria** and **foreign bacteria** that mimic those attributed to experimental strains. Rules are specified using a simple scripting language described in [21].

A. State transition functions

In Figure 2 we describe the state transition functions for each of the automata corresponding to a specific cell-type in a state chart like formalism [6]. Red arrows indicate transitions that represent events in the inflammatory pathway depicted in Figure 1 and blue arrows indicate transitions that represent those of the regulatory pathway. Parameters are listed in Table II. Parameter values were assigned according to measurements published in literature when available and default model assumptions explained in [21]. There one can also find a detailed explanation of each automaton and semantic approximations of the model.

III. IMPLEMENTATION

The computation structure of implementation consists of three main components: cells, locations, and message

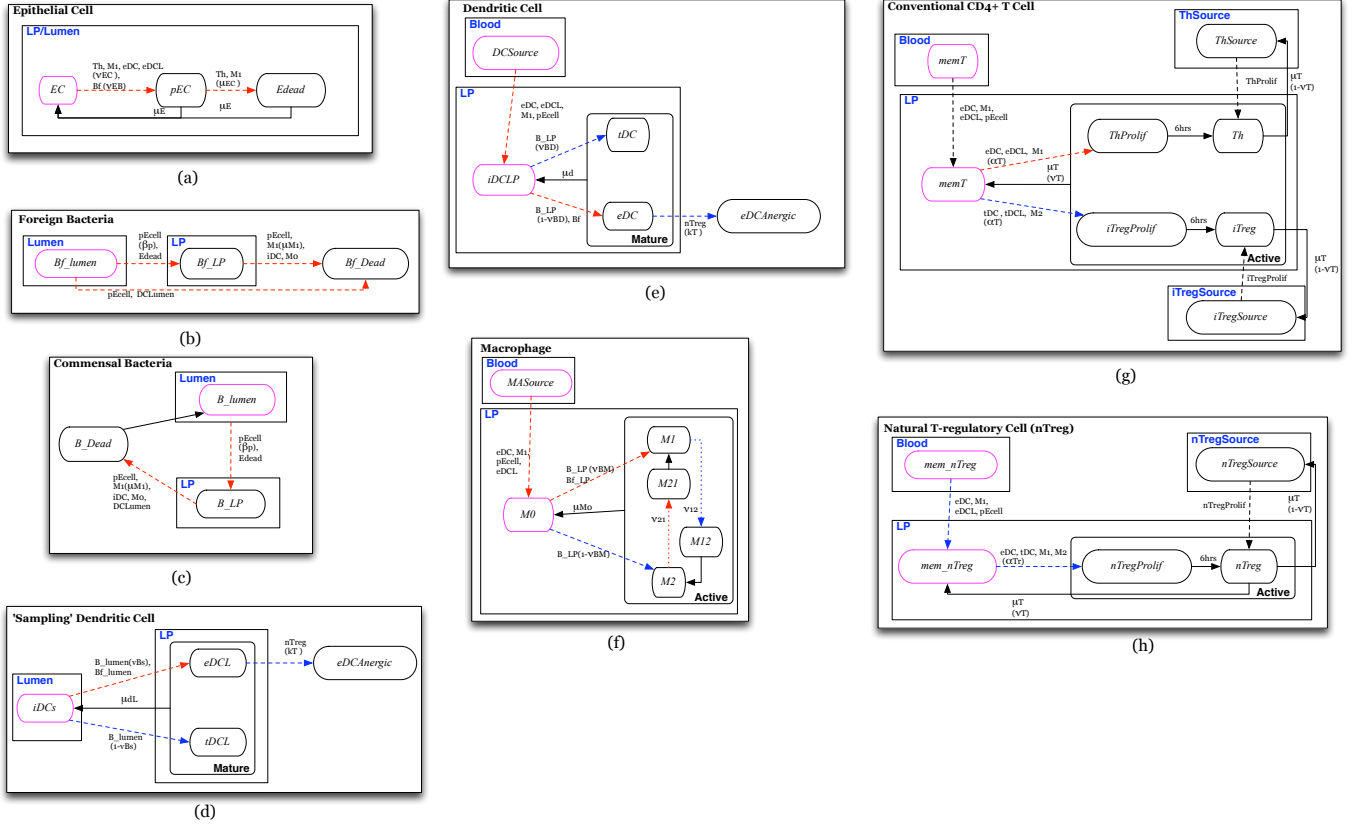


Fig. 2. State transition functions for each of the seven automaton that represent specific cell-types. Each individual is represented by one of the seven automaton. Ovals represent states of the automaton. Solid arrows represent time-dependent transitions labelled with the time in one state before transitioning to another. The dashed arrows represent single contact-dependent transitions, labelled with the set of *Interactor* states necessary to induce state transition and, in parenthesis, the probability of transition upon interaction. The default probability is 1. Dotted arrows represent multicontact-dependent state transitions and are labeled with the function that determines the probability of interaction. Unlabelled solid arrows indicate that transition automatically occurs at the next update. States outlined in pink indicate the initial state that determines which automaton a cell will be. States are depicted in boxes labelled with blue text that indicate the specific *Location* to which individuals in the state are assigned.

brokers. We assume a parallel system consisting of N cores, or processing elements (PEs). Processing proceeds in the following manner:

Partitioning: Cells and locations are partitioned into N groups denoted by C_1, C_2, \dots, C_N and L_1, L_2, \dots, L_N respectively. Currently the distribution is done in a round-robin fashion to allow even load balancing and simpler data management. Each PE also creates a copy of the message broker, denoted by MB_1, MB_2, \dots, MB_N . Each PE then executes the ENISI algorithm (described below) on its local data set (C_i, L_i).

Computing Visit Data: The first phase of the algorithm consists of computing a set of visits for each individual, c_i for the cycle according to the assigned schedule. A light-weight “copy” of each cell (called a *visit message*) is then sent to each location (which may be on a different PE) via the local message broker.

Computing Interactions: Each location receives the visit messages and forms a serial discrete event simulation (DES) by collecting the messages into a time-ordered list of arrive and depart events. Using this data, each location computes

interactions for each individual at that location.

Whether an individual c_j interacts with others in the sublocation is determined by a probability p calculated by one of two functions:

i) *Single contact-dependent* function: $p = 1 - \exp(-\tau \ln(1 - \rho))$, where τ is the duration of contact, and ρ is a constant. This is a pairwise calculation. Hence, if an interaction occurs while performing the calculation on an individual c_j in contact with a neighbor c_k , only c_j will receive the interaction message and potentially change states. A separate interaction probability is then calculated on c_k .

ii) *Multicontact-dependent* function: $p = \left(\frac{aA}{aA + iI}\right)^y$, where A is the total number of neighbors in a state that induces a state change and I is the total number of neighbors in a state that inhibits a state change in c_j . The variables a , i , and y are constants. For each individual that interacts, an *interaction message* is then sent back to the “home” PEs of each cell via the local message broker.

Collecting Interaction Messages: At the end of each cycle, interaction messages for each cell on a PE are merged, processed and the resulting state of each individual automaton

TABLE I
MODEL STATES

State	Description	Initial Number Individuals
Phenotypes		
<i>memT</i>	Resting CD4+ memory T cell	$1 \cdot 10^3$
<i>Th</i>	Active CD4+ T helper cell	0
<i>iTreg</i>	Induced T regulatory cell	0
<i>nTreg</i>	Active natural T regulatory cell	0
<i>mem_nTreg</i>	Resting natural T regulatory cell	0
<i>iDCs</i>	Immature 'sampling' DC in the superficial LP with access to the Lumen	1000
<i>iDCLP</i>	Immature dendritic cell in the LP	1000
<i>eDC</i>	Effector dendritic cell in the LP	0
<i>tDC</i>	Tolerogenic dendritic cell in the LP	0
<i>eDCL</i>	Effector sDC in the lumen	0
<i>tDCL</i>	Tolerogenic sDC dendritic cell in the lumen	0
<i>DCAnergic</i>	Anergic dendritic cell	0
<i>M0</i>	Undifferentiated macrophage	$1 \cdot 10^3$
<i>M1</i>	Activated inflammatory macrophage	0
<i>M12</i>	M2 recently transitioned from M1	0
<i>M21</i>	M1 recently transitioned from M2	0
<i>M2</i>	Activated regulatory macrophage	0
<i>EC</i>	Healthy epithelial cell	10^4 [14]
<i>pEC</i>	Damaged or pro-inflammatory epithelial cell	0
<i>MASource</i>	monocytes: MA precursor	10^5
<i>DCSource</i>	monocytes: DC precursor	10^5
<i>memTSource</i>	memory T cell in blood	10^4
<i>ThSource</i>	Potential child cell from a proliferating Th	$5 \cdot 10^5$
<i>iTregSource</i>	Potential child cell from a proliferating iTreg	$5 \cdot 10^5$
Locations		
<i>B_lumen</i>	Commensal bacterium in the lumen	1000
<i>Bf_lumen</i>	Foreign bacterium in the lumen	30
<i>B_LP</i>	Commensal bacterium in the LP	0
<i>Bf_LP</i>	Foreign bacterium in the LP	0
Death		
<i>Edead</i>	Killed epithelial cell	0
<i>B_dead</i>	Killed commensal bacterium	0
<i>Bf_dead</i>	Killed foreign bacterium	0

is updated according to its type-specific transition function. If an individual c_j received a message it then transitions from its current state s_j to the next state in its automaton, x , with the probability p_{s_jx} .

This synchronous update at the end of each cycle assumes that any changes in behavior that result from the state transition do not take place until the next cycle. As each cycle represents six simulation hours, the synchronous update assumes a six hour delay between a cell receiving the signal to differentiate and actual expression of cytokines or movement-mediating factors, such as integrins, that will affect subsequent movement, contacts, and effects on neighboring cells.

A pseudocode version of the algorithm is show below as **Algorithm 1**. All the PEs in the system are synchronized after each simulation phase above. This guarantees that each location has received all the data required to form a DES and each cell has all the data needed to compute its new state.

TABLE II
PARAMETER VALUES

Symbol	Parameter	Value
Birth/death		
μ_E	Turnover time of epithelial cells	12hrs[14]
μ_T	Time a T cell remains active	5days [16]
μ_{M0}	Time a macrophage remains active	75 days
μ_d	Time a dendritic cell remains active	1 day [15]
μ_{dL}	Time a sDC remains active	1 day [15]
μ_{ce}	Probability that <i>pEcell</i> is killed by inflammatory factors	
p_T	Average number of daughter cells produced by a proliferating T cell	500 [20]
p_{Tr}	Average number of daughter cells produced by a proliferating nTreg	0
Migration		
ϵ_r	Average number of monocytes recruited by a single <i>eDC</i> , <i>M1</i> , or <i>pEcell</i>	10
ϵ_t	Average number of resting T cells recruited by a single <i>eDC</i> , <i>M1</i> , or <i>pEcell</i>	10
β_p	Probability that bacteria will enter the lumen upon contact with a <i>pEcell</i>	1
Contact/interactions		
α_T	Probability of memory T cell stimulation	1
α_{Tr}	Probability of memory nTreg stimulation	1
ν_T	fraction of active T cells that become memory T cells	0.1 [13]
ν_{12}	Probability that M_1 switches to M_2	$\left(\frac{a_1 R}{a_1 R + i_1 N}\right)^{y_1}$
ν_{21}	Probability that M_2 switches to M_1	$\left(\frac{a_2 N}{i_2 R + a_2 N}\right)^{y_2}$
a_1	co-efficient of ν_{12} for activators	1
i_1	co-efficient of ν_{12} for inhibitors	1
y_1	exponent of ν_{12}	4
a_2	co-efficient of ν_{21} for activators	1
i_2	co-efficient of ν_{21} for inhibitors	4
y_2	exponent of ν_{21}	
ν_{BM}	probability that microfloral bacteria induces inflammatory phenotype in macrophages	0
ν_{BD}	probability that microfloral bacteria induces inflammatory phenotype in dendritic cells	0
ν_{Bs}	probability that microfloral bacteria induces inflammatory phenotype in 'sampling' dendritic cells	0
ν_{EC}	Probability that <i>EC</i> transitions to <i>pEcell</i> upon contact with inflammatory factors	0.05
ν_{EB}	Probability that <i>EC</i> is damaged by microbial toxins	1[17]

The ENISI framework is implemented in C++ and uses the Message Passing Interface (MPI) for distributed processing.

IV. EXAMPLE APPLICATION: EXPLANATION OF *B. hyodysenteriae* ASSOCIATED PATHOGENESIS

B. hyodysenteriae infection is characterized by severe dysentery in which epithelial lining is damaged and bacteria is detected in the LP resulting in fever and bloody diarrhea. Associated with infection is the phenomenon that, following *B. hyodysenteriae* -induced epithelial damage, normally tolerogenic commensal bacteria is able to induce an inflammatory response allowing persistent tissue damage [10].

Simulations with ENISI provide visual outputs in two formats; *i*) a plot of the total number of individuals in each state in each location over time and *ii*) a report of the number

Algorithm 1: A pseudocode description of the parallel version of the ENISI algorithm

```

initialize;
partition data across PEs partition;
for  $t = 0$  to  $T$  increasing by  $\Delta t$  do
  foreach cell  $c_j \in C_i$  do
    send visits to location PEs;
    computeVisits( $j, t$  to  $t + \Delta t$ );
    sendVisits( $MB_i$ );
  Visits  $\leftarrow MB_i$ .retrieveMessages();
  synchronize();
  foreach location  $l_k \in L_i$  do
    compose a serial DES;
    makeEvents( $k$ , Visits);
    turn visit data into events;
    computeInteractions( $k$ );
    Process Events;
    sendOutcomes( $MB_i$ );
   $MB_i$ .retrieveMessages();
  synchronize();
  foreach  $c_j \in C_i$  do
    combine outcomes of multiple interactions;
    updateState( $c_j$ );

```

of individuals in each state that interact with an individual in a user-specified state $s_i \in S$ and induce the state change $s_i \rightarrow x$ over a user-specified time period during the simulation. These counts may then be represented in a number of graphical formats.

Here we demonstrate an application of ENISI by simulating a typical inflammatory response to *B. hyodysenteriae*, an experimental model for chronic immunopathological colon inflammation. We then turn to examples of simulation output to identify a key pathway by which chronic inflammation may persist with continued epithelial cell damage following *B. hyodysenteriae* elimination.

Let κ_s^t be the number of individuals in state s at time t and $\kappa_{[s,u]}^t$ be the number of individuals in state s or u at time t .

In this demonstration, we seek to identify pathways that lead to two different health outcomes following infection, complete recovery and chronic inflammation. *Complete recovery* is a configuration in which $\kappa_{[B_{LP}, B_{fLP}, pE_{cell}, E_{dead}]}^t = 0$ and $\kappa_{[Th, M1, eDC, eDCL]}^t < r$, where r is a threshold value, $t > t_{Bf_dead}$, and t_{Bf_dead} is the time at which the last cell enters the *Bf_dead* state. *Chronic inflammation* is a configuration in which $\kappa_{[B_{LP}, pE_{cell}, E_{dead}]}^t \geq 1$ and $\kappa_{[Th, M1, eDC, eDCL]}^t \geq r$, where $r = 1$.

Parameter values for this demonstration are listed in Table II and were assigned according to published observations of interactions between bacteria of the *Brachyspira* genus and immune cells or were fit to cell population dynamics reported in animal infection models [12], [10]. Parameter space was reduced by simplifying assumptions. For example, commensal strains represented do not induce an inflammatory response leading to the assignment $v_{BM} = v_{BD} = v_{Bs} = 0$. For a more detailed explanation of parameter estimation and assumptions, refer to [21].

Table I gives the number of individuals initially assigned to each of the states to represent an immunologically inactive system at the time of infection.

Figure 3 shows simulated dynamics of certain cell populations over a period of 300 cycles (75 days) under different infection scenarios. The top panel shows expected behavior in a pathogen-free mucosa following population of the lumen by commensal bacteria [18], [9]. Specifically, immune activation occurs indicated by elevated κ_{DC} (not shown) and κ_{Treg} (Figure 3(a)). However there is no inflammatory response nor damaged epithelial cells (Figure 3(c)). This inhibits bacterial invasion in to the LP and macrophages remain unstimulated (Figure 3(b)). The middle panel shows the system response to the addition of 30 individuals in the *Bf_lumen* state, representing *B. hyodysenteriae*, on days 1, 2, and 3. The dynamics observed are in agreement with those seen experimentally in pig infections [12], [10] and generally expected with three distinct phases; *i) the acute inflammation (days 1-6)* marked by an increase in κ_{eDC} (not shown) and κ_{Th} (Figure 3(d)), followed by epithelial damage (Figure 3(f)) that is shortly followed by bacterial invasion in to the LP (not shown). At this time macrophages are stimulated and we see κ_{M1} (Figure 3(e)) rise in conjunction with κ_{Th} (Figure 3(d)) along with increased monocyte recruitment and transient reduction in M2 (Figure 3(e)); *ii) the decline of inflammation (days 7-50)* in which clinical symptoms of epithelial damage and bacterial invasion to the LP subside after 1 week (Figure 3(f)) as the number of inflammatory T cells continues to rise, along with M1, before declining after 2 weeks. This decline occurs in conjunction with pathogen elimination; *iii) the chronic phase (days 51-75)* is marked by continued low level epithelial damage (Figure 3(f)) along with bacterial presence in the LP (not shown). In this phase foreign bacteria has already been removed.

To identify the source of this continued epithelial damage we observed the states of those neighbors that induce the transition $EC \rightarrow pE_{cell}$ for all **epithelial cells** that undergo this transition during the three phases of infection. In Figure 4(a), it can be seen that at all stages of infection, it is individuals occupying the *Th* state that are inducing the most epithelial damage. In Figure 4(b) we report the states of neighbors that induce the transition $memT \rightarrow Th$ showing clearly that, in the chronic phase, it is individuals in the transient state *M21*, an intermediate state between M2 and M1, that are solely responsible for Th stimulation. In this phase, only tolerogenic commensal bacteria is present to activate macrophages. To further demonstrate that it is stimulation of Th by macrophages that drives tissue damage, simulated infections were repeated in the absence of the ability of M1 to induce state change in neighbors of the *memT* state, allowing T cell stimulation to occur only through contact with eDC. The result is the dynamics shown in the bottom panel of Figure 3. In this hypothetical scenario there is a weaker, more rapidly subsiding inflammatory response as ‘sampling’ dendritic cells stimulate T cells. However, dendritic cell activation is short lived and once the pathogen is removed *eDCL* is quickly removed. The reduced κ_{Th} during the acute inflammation phase results in

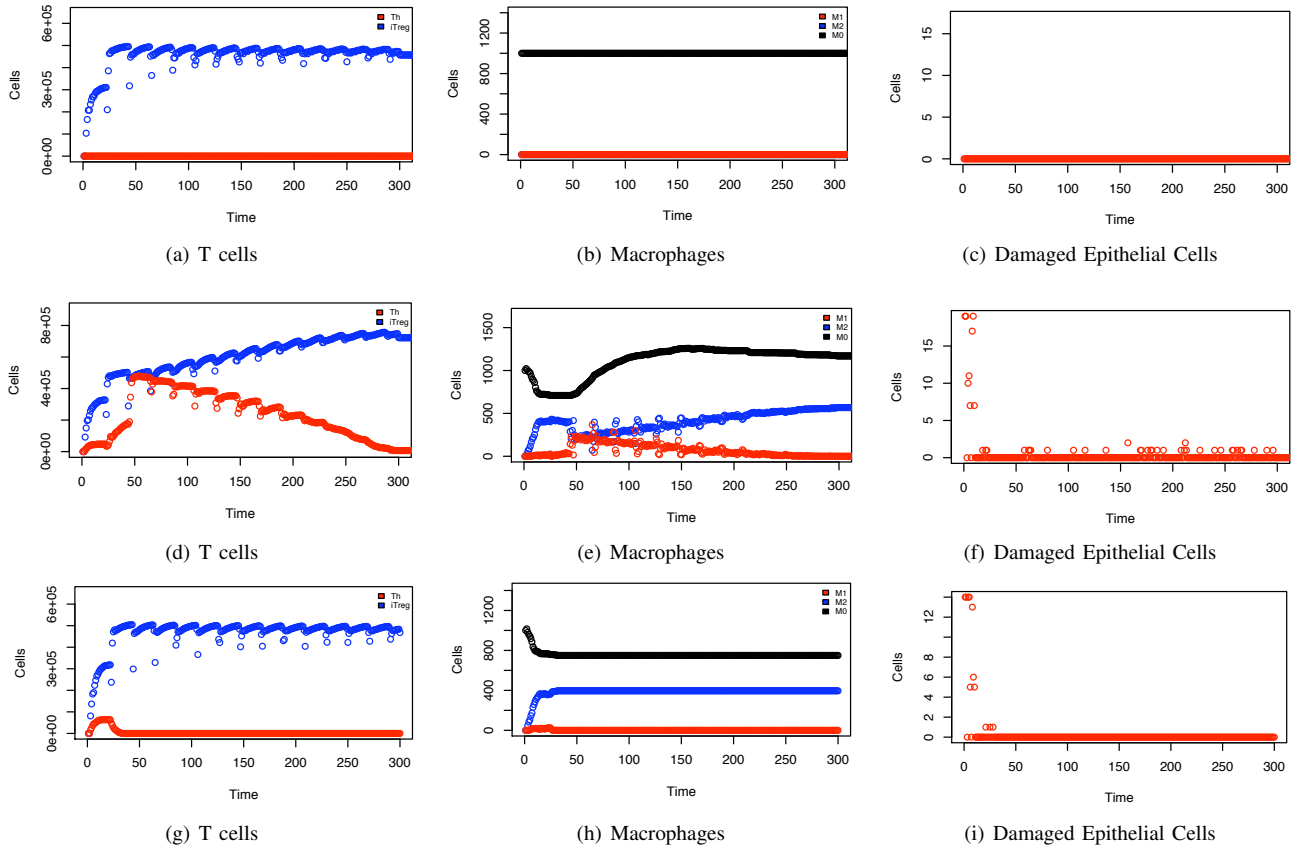


Fig. 3. Dynamics of cell populations over a period of 75 days. Top: no pathogen present, Middle: following infection with *B. hyodysenteriae*, Bottom: following infection with *B. hyodysenteriae* without M1 mediated T cell stimulation. The x-axis is labelled in time units of 6 hours.

less epithelial damage as well as lower inflammatory cytokine concentrations reducing the frequency of $M2 \rightarrow M1$ transitions. This allows a tolerogenic environment to persist.

The conclusion of this simple demonstration is that residual tissue damage following *B. hyodysenteriae* infection occurs through Th1/Th17-mediated cytotoxicity which is stimulated by M1 that has recently transitioned from the M2 phenotype. The presence of M1 is due to two parallel consequences of pathogen presence; *i*) the increase of the Th1/Th17 population that leads to increase of M1-inducing inflammatory cytokines in the tissue, and *ii*) increased damage of the epithelial layer which allows invasion of commensal bacteria. The implication is that commensal bacteria, which directly induces a tolerogenic response, is indirectly responsible for maintaining immunopathological chronic inflammation via macrophage stimulation once the environmental concentration of inflammatory cytokines reaches above a certain threshold.

V. RELEVANCE AND FUTURE DIRECTIONS

Aspects of the presented inflammatory and regulatory immune pathways have been represented in previous models of mucosal infection [1], [22], [4], [5]. The ENISI model is unique in its scope and approach. The model incorporates regulatory mechanisms of both adaptive and innate immunity,

multi-location migration of cells, and cross talk between antigen presenting cells and T cells. In addition, it is mechanism-based explicitly representing each participating cell of the immune pathway. This agent-based approach allows incorporation of spatial effects and randomness of cell-cell and cell-bacteria contact. In the case of colonic inflammation spawned by a small number of pathogen, such randomness is believed to significantly affect the outcome of the system and, therefore, an agent-based model is an appropriate representation [3].

The ENISI algorithm is an extension of one known to scale to large numbers approaching those found in the true system [2]. Large scale models are necessary for immune simulators whose purpose is to reproduce dynamics in a true *in vivo* system that lead to tissue level phenomenon by simulating interactions between individual cells where cell concentrations can reach $10^8/mL$ [8]. It may not be sufficient to simulate the dynamics of a small sample and extrapolate results to the entire organ. To do so is to ignore the non-linear and complex nature of the cell interactions and dynamics by making the assumption of uniform mixing which defeats the purpose of an agent-based approach. ENISI is a unique contribution to the field of immunological tools as an agent-based model of an unprecedented scale, simulating complex interaction and migration of 10^6 individuals over a simulated three month

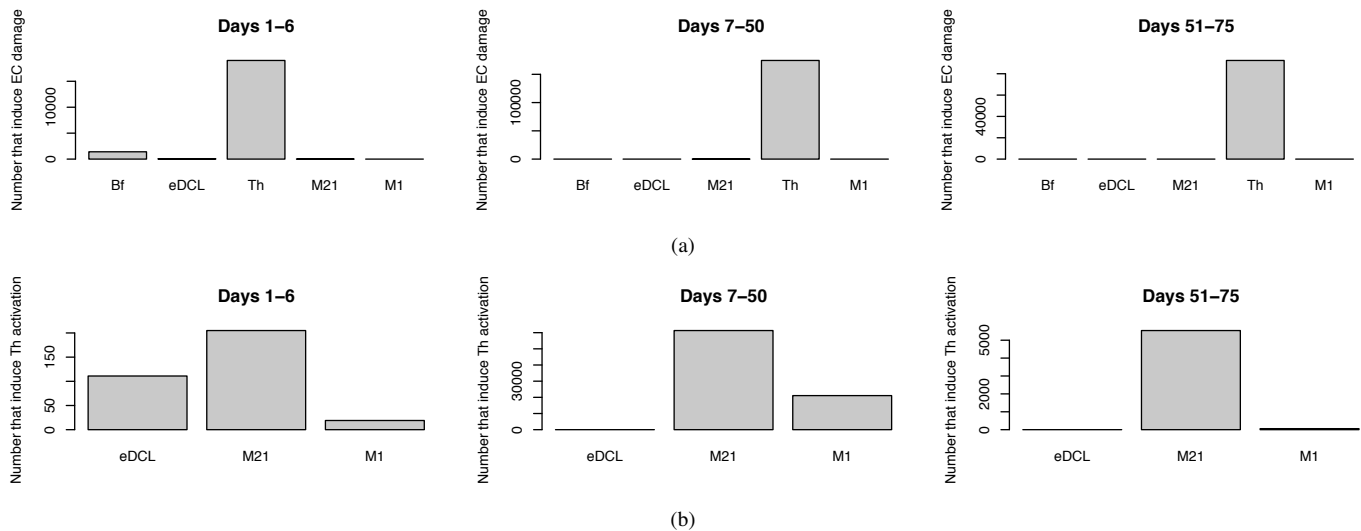


Fig. 4. (a) Histogram of the number of individuals in each state that interact with an **epithelial cell** and induce the transition $EC \rightarrow pEcell$. (b) Histogram of the number of individuals in each state that interact with a **T cell** and induce the transition $memT \rightarrow Th$

period with in one hour.

Though scripting is currently required to create simulation specifications, a graphical user interface is under construction and will be publicly available at <http://www.modelingimmunity.org>. ENISI is an evolving *in silico* system. It is currently being extended to include lymphoid tissues and cytokine-dependent movement. In addition, automata that represent specific bacterial species such as *Helicobacter pylori* and *Escherichia coli* will be included and T cell populations will be further refined in to separate Th1 and Th17 types.

REFERENCES

- [1] J. C. Arciero, G. B. Ermentrout, J. S. Upperman, Y. Vodovotz, and J. E. Rubin. Using a mathematical model to analyze the role of probiotics and inflammation in necrotizing enterocolitis. *PLoS One*, 5(4):e10066, 2010.
- [2] C. Barrett, K. Bisset, S. Eubank, X. Feng, and M. Marathe. Episimemics: an efficient algorithm for simulating the spread of infectious disease over large realistic social networks, 2008.
- [3] Perelson A. Bauer A., Beauchemin C. Agent-based modeling in host-pathogen systems: The successes and challenges. *Information Sciences*, 179:1379–1389, 2009.
- [4] M. J. Blaser and D. Kirschner. Dynamics of helicobacter pylori colonization in relation to the host response. *Proc Natl Acad Sci U S A*, 96(15):8359–64, 1999.
- [5] M. J. Blaser and D. Kirschner. The equilibria that allow bacterial persistence in human hosts. *Nature*, 449(7164):843–9, 2007.
- [6] D. Gery and E. Harel. Executable object modeling with statecharts. *Computer*, 30(7):31–42, 1997.
- [7] S. Gordon and P. R. Taylor. Monocyte and macrophage heterogeneity. *Nat Rev Immunol*, 5(12):953–64, 2005.
- [8] A. T. Haase. Population biology of hiv-1 infection: Viral and cd4(+) t cell demographics and dynamics in lymphatic tissues. *Annual Review of Immunology*, 17:625–656, 1999.
- [9] D. A. Hill and D. Artis. Intestinal bacteria and the regulation of immune cell homeostasis. *Annu Rev Immunol*, 28:623–67, 2010.
- [10] R. Hontecillas and J. Bassaganya-Riera. Peroxisome proliferator-activated receptor gamma is required for regulatory cd4+ t cell-mediated protection against colitis. *J Immunol*, 178(5):2940–9, 2007.
- [11] A. Iwasaki. Mucosal dendritic cells. *Annual Review of Immunology*, 25:381–418, 2007.
- [12] R. Jonasson, M. Andersson, T. Rasback, A. Johannisson, and M. Jensen-Waern. Immunological alterations during the clinical and recovery phases of experimental swine dysentery. *J Med Microbiol*, 55(Pt 7):845–55, 2006.
- [13] S. M. Kaech and R. Ahmed. Immunology: CD8 T cells remember with a little help. *Science*, 300(5617):263–5, 2003.
- [14] D. Kelly, J. I. Campbell, T. P. King, G. Grant, E. A. Jansson, A. G. Coutts, S. Pettersson, and S. Conway. Commensal anaerobic gut bacteria attenuate inflammation by regulating nuclear-cytoplasmic shuttling of ppar-gamma and rela. *Nat Immunol*, 5(1):104–12, 2004.
- [15] A. Lanzavecchia and F. Sallusto. Regulation of t cell immunity by dendritic cells. *Cell*, 106(3):263–6, 2001.
- [16] A. L. Marzo, K. D. Klonowski, A. Le Bon, P. Borrow, D. F. Tough, and L. Lefrancois. Initial t cell frequency dictates memory cd8+ t cell lineage commitment. *Nat Immunol*, 6(8):793–9, 2005.
- [17] R. Naresh, Y. Song, and D. J. Hampson. The intestinal spirochete brachyspira pilosicoli attaches to cultured caco-2 cells and induces pathological changes. *PLoS One*, 4(12):e8352, 2009.
- [18] S. C. Ng, M. A. Kamm, A. J. Stagg, and S. C. Knight. Intestinal dendritic cells: their role in bacterial recognition, lymphocyte homing, and intestinal inflammation. *Inflamm Bowel Dis*, 16(10):1787–807, 2010.
- [19] Y. Onishi, Z. Fehervari, T. Yamaguchi, and S. Sakaguchi. Foxp3(+) natural regulatory t cells preferentially form aggregates on dendritic cells in vitro and actively inhibit their maturation. *Proceedings of the National Academy of Sciences of the United States of America*, 105(29):10113–10118, 2008. 330BB Times Cited:23 Cited References Count:39.
- [20] F. Sallusto, J. Geginat, and A. Lanzavecchia. Central memory and effector memory t cell subsets: function, generation, and maintenance. *Annu Rev Immunol*, 22:745–63, 2004.
- [21] K.V. Wendelsdorf, J. Bassaganya-Riera, K. Bisset, S. Eubank, R. Hontecillas, and M. Marathe. Enteric immunity simulator: A tool for in silico study of gut immunopathologies. *NDSSL TR-11-072*, <http://modelingimmunity.vbi.vt.edu/modeling/enisi/>, 2011.
- [22] J. E. Wigginton and D. Kirschner. A model to predict cell-mediated immune regulatory mechanisms during human infection with mycobacterium tuberculosis. *J Immunol*, 166(3):1951–67, 2001.